Supporting Information

A Naphthalimide-Based Turn-on Fluorescent Probe for Peroxynitrite Detection and Imaging in Living Cells

Xiling Liu,[b] Fangyuan Gu,[c] Xinyi Zhou,[c] Wei Zhou, *[a] Shuping Zhang,[b] Lei Cui,[c] Ting Guo *[a]

[a] College of Pharmaceutical Sciences, Southwest University, Chongqing 400715, China
[b] College of Science, University of Shanghai for Science and Technology, Shanghai 200093, China
[c] College of Science, Shanghai University, Shanghai 200444, China

Contents

1. Experiment 1
1.1 Preparation of reactive oxygen species (ROS) 1
1.2 The limit of detection (LOD) of HCA-OH 1
2. UV-Vis absorption spectra 2
3. Time-dependent changes in the fluorescence intensity 3
4. LC-MS spectroscopy 4
5. Effects of pH 5
6. Cytotoxicity assays 5
7. Crystal data and structure refinement for HCA-OH 6
8. Optimization result "coordinate data" calculated by Density Functional Theory (TD-DFT) 6
9. NMR and HRMS spectra 9

1. Experiment

1.1 Preparation of reactive oxygen species (ROS)

Peroxynitrite solution ($ONOO^-$) was synthesized as reported literature. Briefly, hydrogen peroxide (0.7 M, 1.5 mL) was acidified with hydrochloric acid (0.6 M, 1.5 mL) under ice-water bath, sodium nitrite (0.6 M, 3 mL) and sodium hydroxide (1.5 M, 3 mL) was added simultaneously in 1-2 s. The solution turned bright yellow. Then a small amount of MnO_2 was added to remove excess hydrogen peroxide. The prepared $ONOO^-$ package is stored at -20 ^oC. The concentration of peroxynitrite was estimated by using an extinction coefficient of 1670 M^{-1} cm^{-1} at 302 nm. C_{ONOO^-} = (Abs302 nm / 1670)* dilution factor.[1] Hydrogen peroxide (H_2O_2), hypochlorite (ClO^-), sodium nitrite ($NaNO_2$) and tert-butyl hydroperoxide (t-BuOOH) were delivered from commercial aqueous solutions, respectively. Nitric oxide (NO) was used from a stock solution prepared by sodium nitroprusside. Singlet oxygen ($^1O_2$) was generated in situ by addition of the H_2O_2 stock solution into a solution containing 10 equiv. of HClO. Superoxide solution ($O_2^{\bullet-}$) was prepared by adding KO_2 into dry dimethyl sulfoxide (DMSO) and stirring vigorously for 10 min. Hydroxyl radicals (•OH) was generated by Fenton reaction, $FeCl_2$ was added in the presence of 10 equiv. H_2O_2.

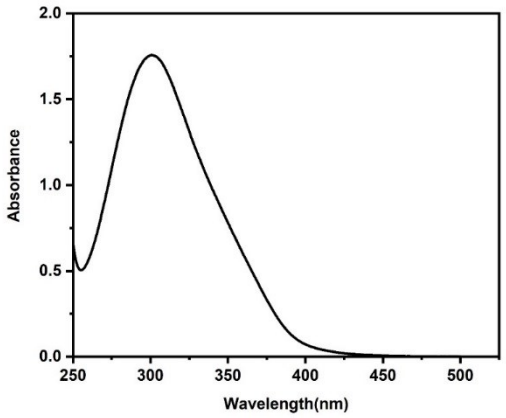

Fig. S1 Absorption spectrum of peroxynitrite

1.2 The limit of detection (LOD) of HCA-OH

The emission spectrum of free **HCA-OH** in PBS buffer (10 mM, pH 7.4, containing 1% DMSO) was collected for 11 times to confirm the background noise σ. The probe noise can be calculated from fluorescence signals in solution without $ONOO^-$ using the root-mean-square (σ), we took 11 data points to obtain the average value before treated with $ONOO^-$.

$$Vx^2 = \Sigma\ (yi - y)^2$$

Where *yi* is the average value from calculation and *y* is the measured data point. The σ noise is calculated as

$$\sigma = \sqrt{Vx^2/N}$$

Where N is the number of data points used for the average value.

$$LOD = 3\sigma/K$$

The linear regression curve was then fitted according to the data in the range of $ONOO^-$ from 10 to 80 μM and obtained the slope of the curve (7.83 μM). The detection limit was determined to be 49.7 nM, which facilitate the quantitative detection of $ONOO^-$ in the complex environment.[2]

2. UV-Vis absorption spectra

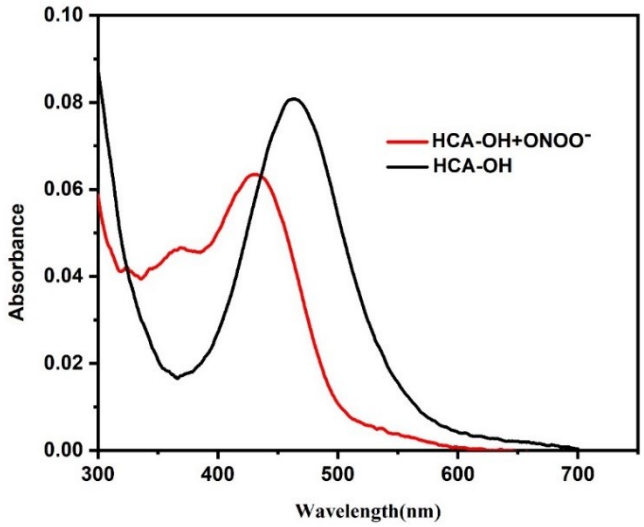

Fig. S2 UV -Vis absorption spectra of **HCA-OH** (black), **HCA-OH** with $ONOO^-$ (red line). The final concentration of the probe was 10 μM and $ONOO^-$ concentrations was 50 μM. Data was acquired in 10 mM PBS buffer (pH 7.4, 1% DMSO) after incubation at 37 ℃ for 20 min.

3. Time-dependent changes in the fluorescence intensity

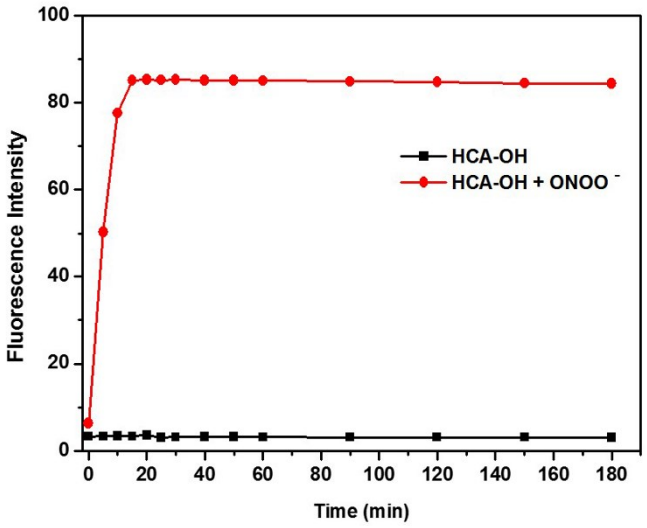

Fig. S3 Time-dependent changes in the fluorescence intensity of **HCA-OH** (black line: 0 μM $ONOO^-$, red line: 30 μM $ONOO^-$). The excitation and emission wavelength were 460 nm and 548 nm, respectively.

4. LC-MS spectroscopy

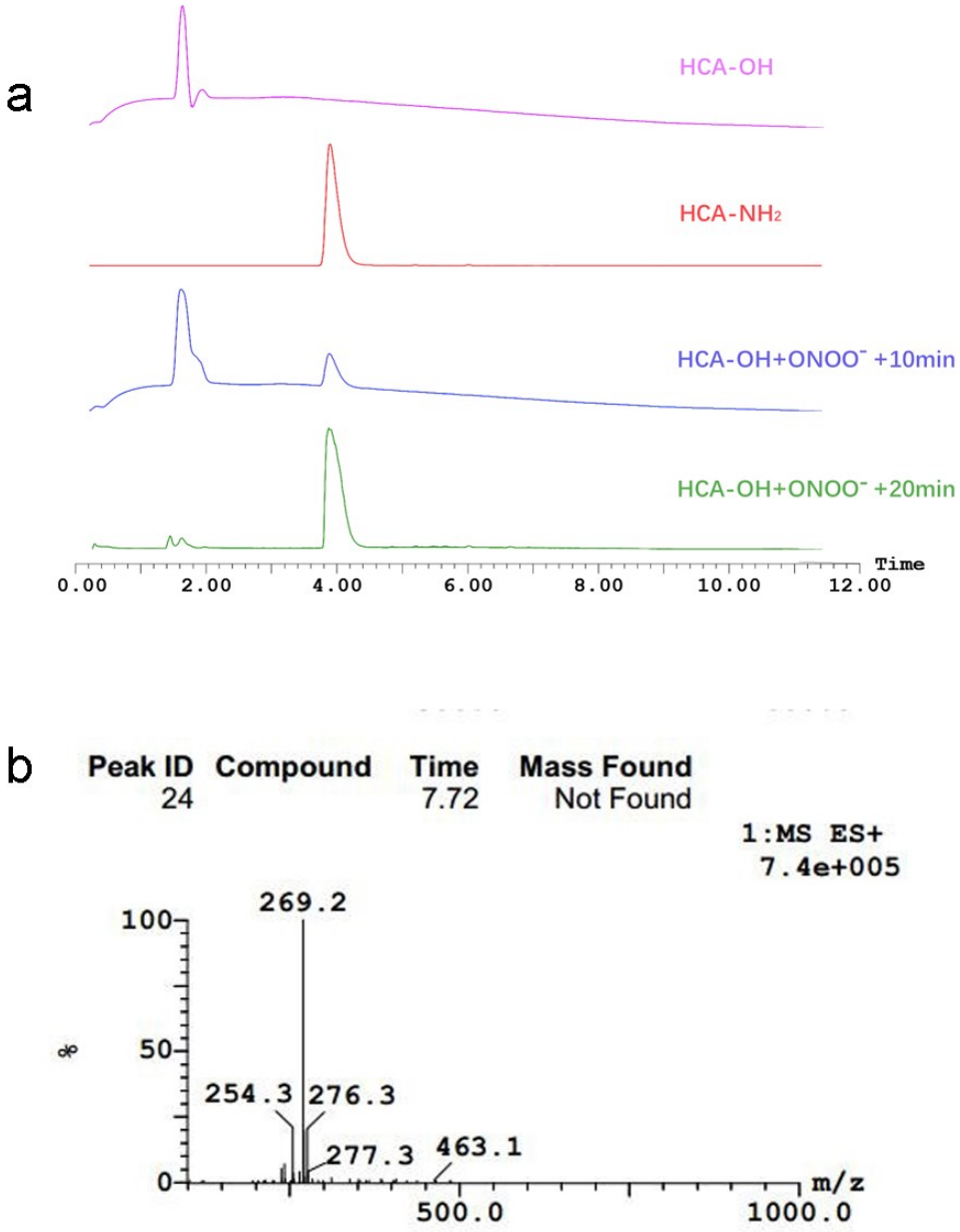

Fig. S4 (a) HPLC traces of **HCA-OH** (purple line), **HCA-NH$_2$** (red line), **HCA-OH** reaction with ONOO$^-$ for 10 min (blue line) and 20 min (green line). (b) ESI-MS spectrum of **HCA-OH** after treated with ONOO$^-$.

5. Effects of pH

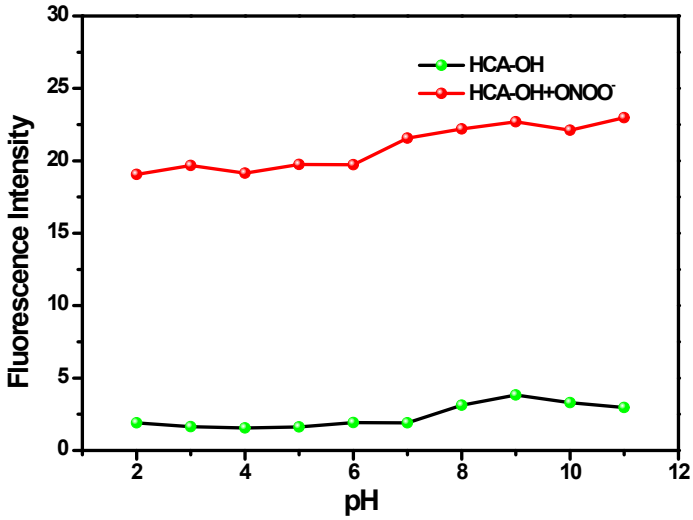

Fig. S5 Fluorescence intensity changes of **HCA-OH** (10 μM) towards $ONOO^-$ (10 μM) in PBS buffer with 1% DMSO under different pH conditions (2.0, 3.0, 4.0, 5.0, 6.0, 7.0, 8.0, 9.0, 10.0, 11.0). The excitation and emission wavelength were 460 nm and 548 nm, respectively.

6. Cytotoxicity assays

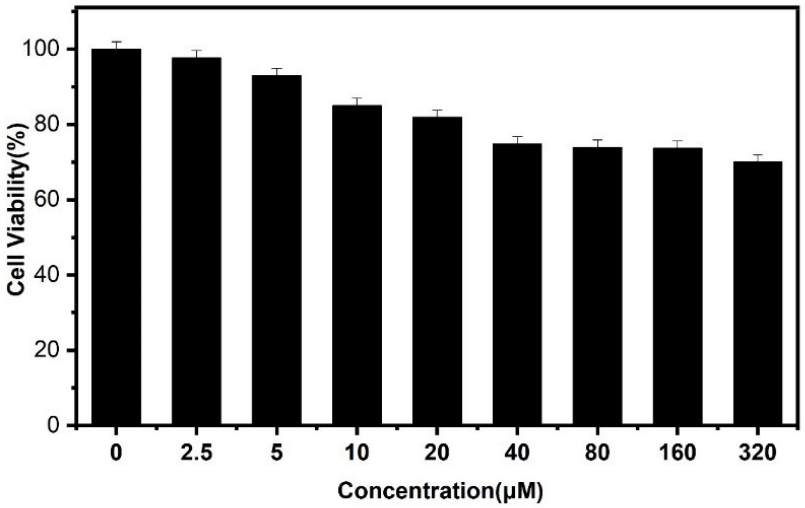

Fig. S6 MTT assays of HepG2 cells

7. Crystal data and structure refinement for HCA-OH

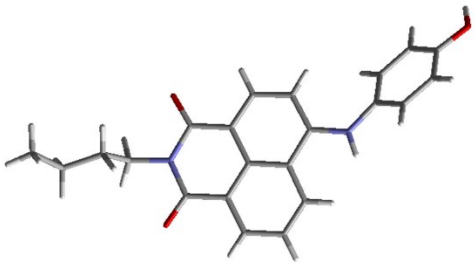

Fig. S7 The crystal structure of **HCA-OH**

Table S1 Crystal data and structure refinement for **HCA-OH**

Compound	**HCA-OH**
Empirical formula	C_{22} H_{22} N_2 O_4
CCDC	1974831
Formula weight	378.41
Crystal system, space group	Monoclinic, $P2_1/c$
Unit cell dimensions (Å, °)	a =13.7287(13) Å a= 90°. b=18.656(2) Å b= 105.962 (6)°. c== 7.4592(7) Å g = 90°.
Volume/ Å^3	1836.8(3) Å^3
Z, Calculated density	4, 1.368 Mg/m^3
Absorption coefficient/mm^{-1}	0.493
F (000)	800
Theta range for data collection/	2.913 to 52.995.
Goodness-of-fit on F^2	0.960
Final R indices [I>2σ]	R1 = 0.0616, wR2 = 0.1407
Large diff. peak and hole/e Å^{-3}	0.235 and -0.236 e.

8. Optimization result "coordinate data" calculated by Density Functional Theory (TD-DFT)

Table S2 Density Functional Theory (TD-DFT) optimized coordinate data

Ground state (S_0) :

Standard orientation:

Center Number	Atomic Number	Atomic Type	Coordinates (Angstroms) X	Y	Z
1	6	0	2.176516	-0.812352	-1.000887
2	6	0	0.833450	-0.310541	-0.977437
3	6	0	-0.218009	-1.094082	-1.477238
4	6	0	0.565784	0.987011	-0.442086
5	6	0	1.626995	1.776242	0.067336
6	6	0	2.975005	1.244910	0.030579
7	6	0	1.351145	3.036721	0.590209
8	1	0	2.169364	3.647265	0.984053
9	6	0	0.041924	3.519015	0.616908
10	6	0	-1.003795	2.756402	0.121421
11	6	0	-0.760783	1.483823	-0.418224
12	6	0	-1.814676	0.661707	-0.946212
13	6	0	-1.552962	-0.571639	-1.447331
14	1	0	-2.355483	-1.202772	-1.841710
15	1	0	-0.161036	4.510203	1.035430
16	1	0	-2.027356	3.141470	0.151531
17	1	0	-0.025555	-2.067936	-1.877693
18	7	0	3.233870	0.003774	-0.480661
19	7	0	-3.173114	1.210120	-0.918445
20	1	0	-3.478647	1.385296	-1.854729
21	6	0	-4.103973	0.288774	-0.273282
22	6	0	-4.809312	-0.644977	-1.029322
23	6	0	-4.291931	0.348910	1.105404
24	6	0	-5.699333	-1.517879	-0.408265
25	1	0	-4.660835	-0.693173	-2.113236
26	6	0	-5.182495	-0.522337	1.726522
27	1	0	-3.739155	1.083887	1.698559
28	6	0	-5.885728	-1.455552	0.969811
29	1	0	-6.250723	-2.253186	-1.002616
30	1	0	-5.332961	-0.475089	2.809217
31	6	0	3.908701	-0.800045	0.560693
32	6	0	5.348489	-1.056468	0.186858
33	1	0	3.359934	-1.756367	0.675477
34	1	0	3.849266	-0.246334	1.519221
35	6	0	6.065008	-1.881599	1.239953
36	1	0	5.390941	-1.586992	-0.792098
37	1	0	5.879499	-0.082546	0.077579
38	6	0	7.506556	-2.137670	0.867156
39	1	0	6.020881	-1.350261	2.219347

40	1	0	5.534885	-2.853835	1.371605
41	1	0	8.009891	-2.742158	1.650442
42	1	0	7.572080	-2.688973	-0.094496
43	1	0	8.059837	-1.181373	0.755689
44	8	0	3.962946	1.995141	0.508361
45	8	0	2.448011	-2.008984	-1.491825
46	8	0	-6.787754	-2.338278	1.609534
47	1	0	-7.685214	-2.057673	1.438207

Excited state (S_1) :

Standard orientation:

Center Number	Atomic Number	Atomic Type	Coordinates (Angstroms) X	Y	Z
1	6	0	-1.380305	2.177788	0.051124
2	6	0	-0.898273	1.006176	-0.578418
3	6	0	-1.699636	0.050207	-1.262358
4	6	0	-0.504581	3.047067	0.713123
5	6	0	0.520405	0.735786	-0.540025
6	6	0	1.377769	1.634668	0.143960
7	6	0	0.856677	2.784815	0.770126
8	6	0	2.816041	1.379106	0.208610
9	6	0	2.478858	-0.703374	-1.134734
10	6	0	1.047376	-0.420142	-1.179509
11	6	0	0.197614	-1.314052	-1.864991
12	6	0	-1.164762	-1.072044	-1.910573
13	1	0	-1.827889	-1.751770	-2.439595
14	1	0	0.638967	-2.181103	-2.341465
15	1	0	-0.902972	3.941011	1.186892
16	1	0	1.547554	3.444835	1.281913
17	1	0	-2.439166	2.414755	0.020736
18	8	0	3.608846	2.116187	0.807270
19	8	0	2.986873	-1.705562	-1.656463
20	7	0	3.281849	0.231710	-0.458859
21	6	0	4.726694	-0.028403	-0.416844
22	6	0	5.140416	-0.867606	0.797188
23	1	0	5.223453	0.942976	-0.388258
24	1	0	4.982640	-0.550720	-1.340313
25	6	0	6.651251	-1.125882	0.837622
26	1	0	4.829709	-0.342901	1.709605
27	1	0	4.601248	-1.823049	0.765490
28	6	0	7.083307	-1.965497	2.044310

29	1	0	6.959065	-1.632466	-0.088343
30	1	0	7.183953	-0.164307	0.852462
31	1	0	8.166816	-2.133963	2.050522
32	1	0	6.817175	-1.469405	2.985941
33	1	0	6.592906	-2.946871	2.038106
34	7	0	-3.133786	0.271323	-1.361131
35	1	0	-3.471516	0.814668	-2.152310
36	6	0	-4.063482	-0.138329	-0.499663
37	6	0	-5.446695	0.174064	-0.735905
38	6	0	-3.719948	-0.899107	0.670798
39	6	0	-6.417633	-0.243375	0.137222
40	1	0	-5.714012	0.746642	-1.618164
41	6	0	-4.696477	-1.308179	1.536393
42	1	0	-2.678958	-1.131483	0.845337
43	6	0	-6.056278	-0.989367	1.285763
44	1	0	-7.461768	-0.005317	-0.047195
45	1	0	-4.457903	-1.880108	2.425841
46	8	0	-6.953455	-1.427873	2.177582
47	1	0	-7.853888	-1.160586	1.926304

---

9. NMR and HRMS spectra

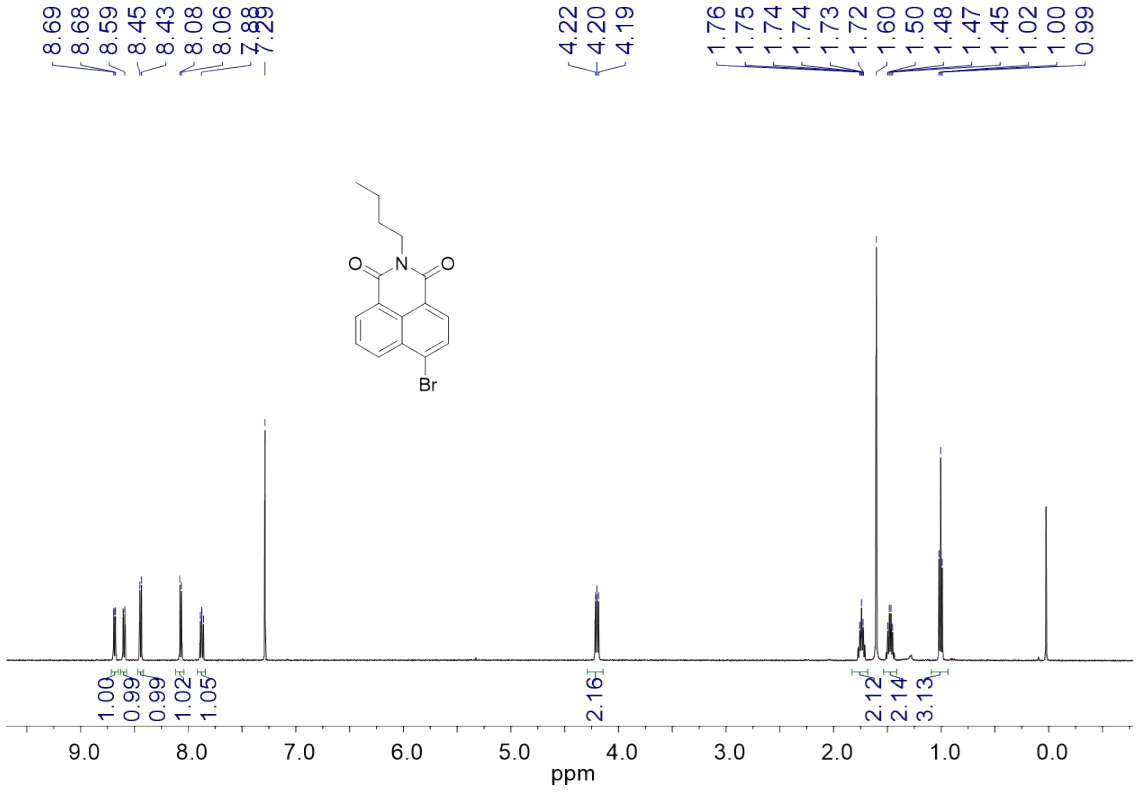

Fig. S8 The ^{1}H-NMR spectrum of compound **1**

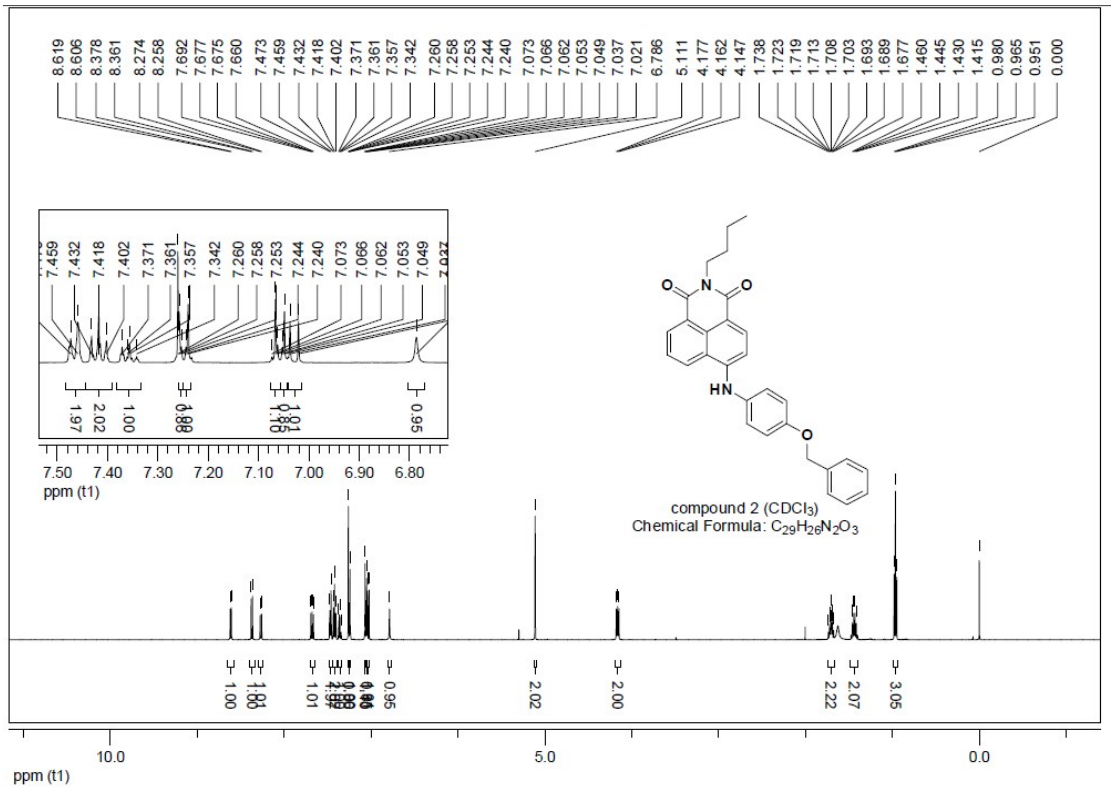

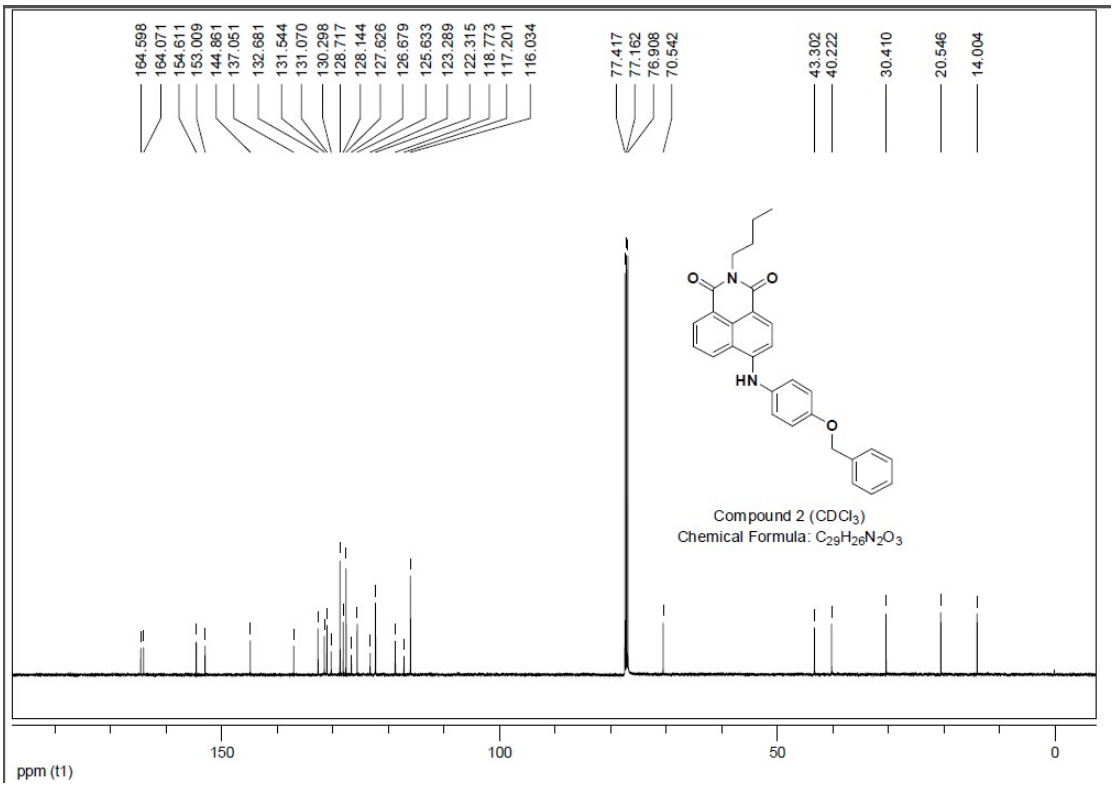

Fig. S9 The ^{1}H-NMR and ^{13}C- NMR spectrum of compound **2**

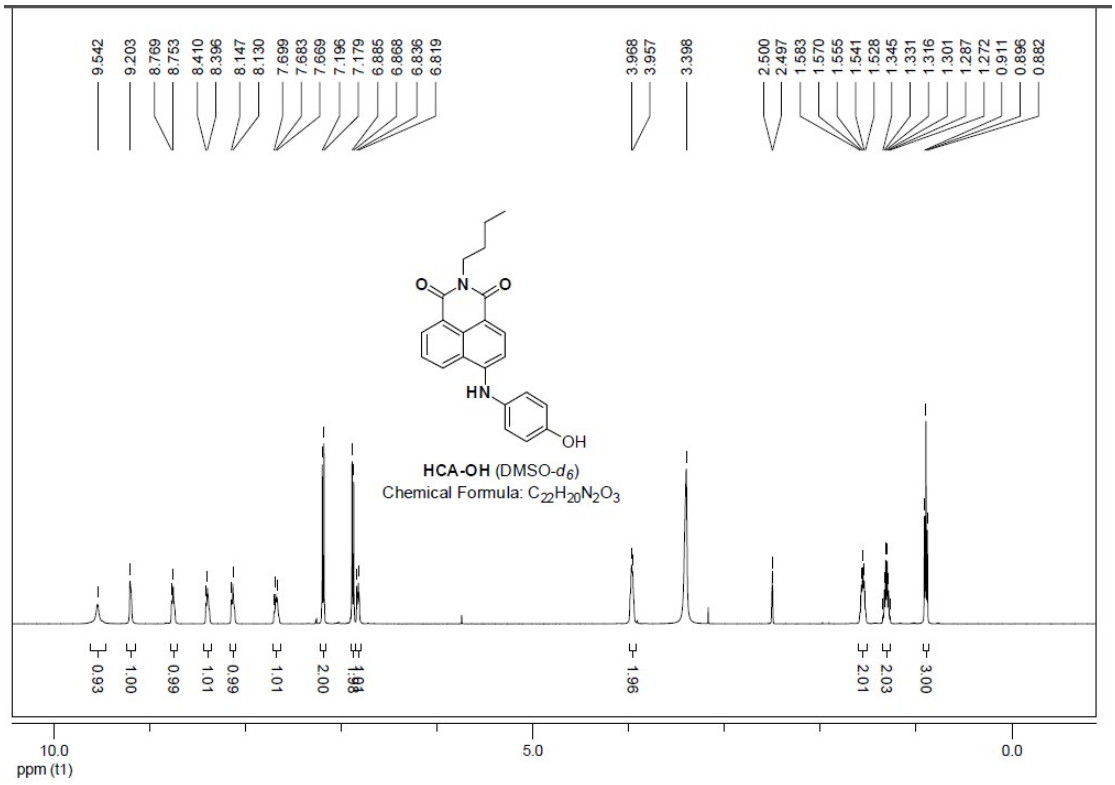

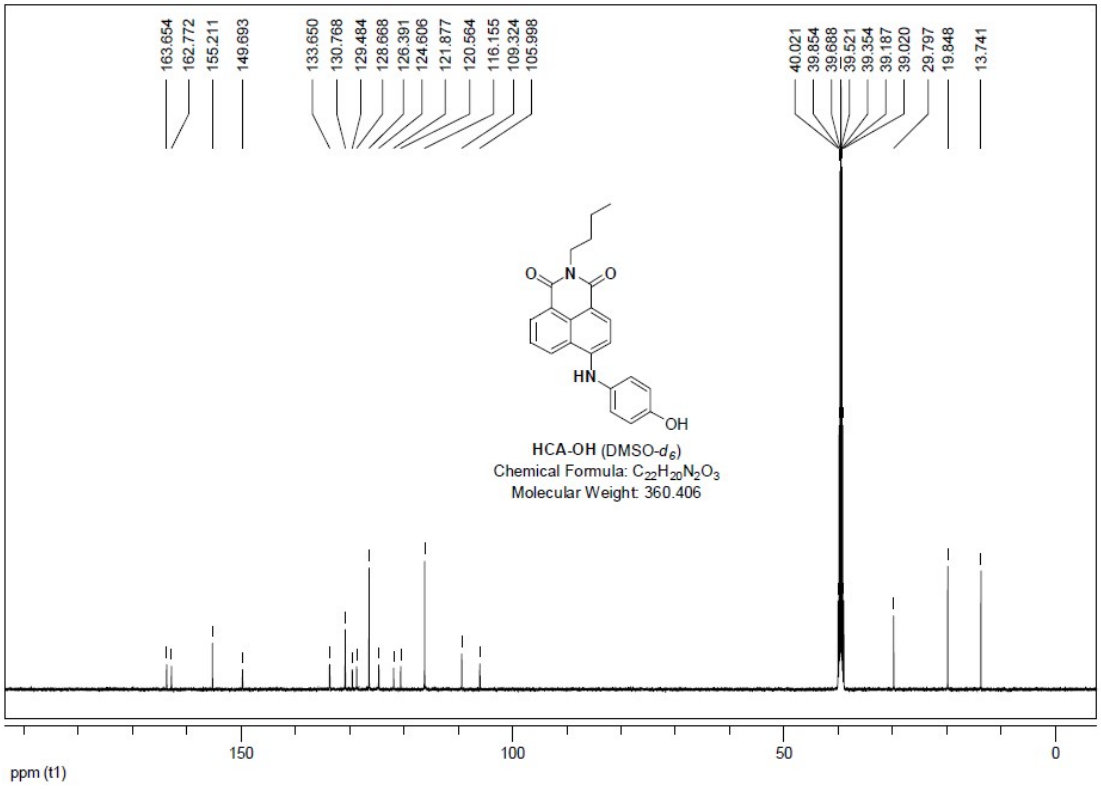

Fig. S10 The ^{1}H-NMR and ^{13}C-NMR spectrum of **HCA-OH** in DMSO-d_6

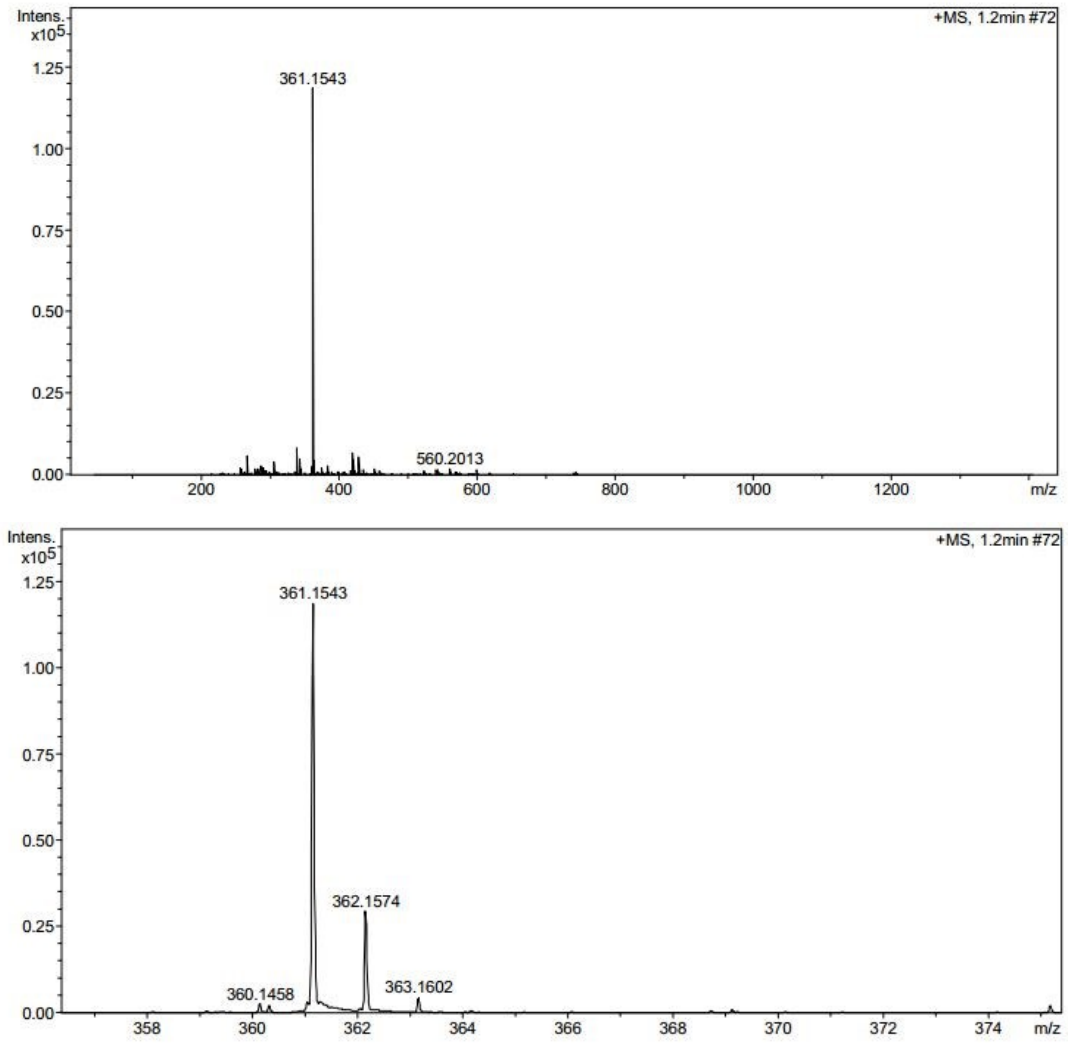

Fig. S11 HR-MS of **HCA-OH**

1. J. S. Hu, C. Shao, X. Wang, X. Di, X. Xue, Z. Su, J. Zhao, H. L. Zhu, H. K. Liu and Y. Qian, Imaging Dynamic Peroxynitrite Fluxes in Epileptic Brains with a Near-Infrared Fluorescent Probe. *Advanced Science*, **2019**, 6(15), 1900341.

2. P. J. Ogren, A. Meetze and W. C. Duer, The Limit of Detection in Generalized Least-Squares Calibrations: An Example Using Alprazolam Liquid Chromatography-Tandem Mass Spectrometry Data. *Journal of Analytical Toxicology*, **2009**, 33(3):129-142.